Fourth International Symposium on Marine Propulsors
smp'15, Austin, Texas, USA, June 2015

Integrated Design of Asymmetric Aftbody and Propeller for an Aframax Tanker to Maximize Energy Efficiency

Jie Dang[1], Chen Hao[2], Luis Rueda[1] and Harry Willemsen[1]

[1] Maritime Research Institute Netherlands, 2 Haagsteeg, 6708PM, Wageningen, The Netherlands

[2] Guangzhou Shipyard International Company Ltd., 40 South Fangcun Road, Guangzhou 510382, China

ABSTRACT

With the implementation of the EEDI, energy saving and emission reduction of ships, especially merchant ships, become more and more important. To achieve high efficiency and low emissions, recently Energy Saving Devices (ESDs) have been re-studied and installed to many ships, both new buildings and also retrofits. Various ESDs, including new concepts, have been tested in model scale and large improvements on energy efficiency have been confirmed. However due to the fact that most ESDs are fitted in the wake field, the performance of the ESDs is influenced by scale effects. For the operators, the fouling and the structure integration of the ESD's with the hull are the important issues to make decisions on applying ESDs to their ships.

Distinguished from the ESDs where extra 'appendages' have to be added in front of and/or behind a propeller, an asymmetric aftbody can also change the flow towards the propeller without appendages. The wake with pre-swirl generated by an asymmetric aftbody is in general more uniform than that by an ESD (such as a pre-stator with finite blades) and with almost no penalty on the ship's resistance. By integrating a propeller, a ship with asymmetric aftbody can be designed so that the hull-propeller interaction is optimized for its total propulsive efficiency and the required shaft power is minimized at given speed.

In this paper, discussions have been given on the optimization procedure by using the Computational Fluid Dynamics (CFD) towards a fully-integrated hull-propeller design to maximize the energy efficiency of a single screw ship. Comparative model tests, carried out with optimized symmetric and asymmetric ships, showed more than 6% gain in efficiency with a moderate asymmetric aftbody, without detriments to its course stability.

Keywords

Energy saving, Propulsion, Hull form, Asymmetric aftbody.

1 INTRODUCTION

Design for the powering performance of ships has been experienced continuous improvements on both hull form design and propulsor design. On one side, the hull forms are designed to accommodate specific propulsors, that result in hull forms which differ a ship with a single screw from a ship with multiple screws; a ship with azimuthing thrusters or pods from a ship with water jet systems. On the other side, the propulsors are also tailored for the wake fields of hull form designs, called the wake-adapted propeller designs (Oosterveld 1970). Except that cares have been taken in the contemporary hull form designs to achieve better wake fields at the propeller for better cavitation performance and to lead more viscous wake into the propeller disc to increase hull efficiency, a real 'propeller-adapted' hull form design has not yet been fully developed.

For many decades, MARIN has been dedicated working on developing sophisticated CFD-aided optimization tools and procedures to design both hull forms and propeller geometries, in order to achieve fully-integrated designs with both maximized propulsive efficiency and comfort for ships. It started from the optimization method for the resistance and the wake quality; for the shaft power based on series propellers (Ploeg & Raven, 2010); for the shaft power with actual design propellers by using RANS-BEM coupling technique and recently developed into optimization procedures where fully-integrated hull form and propeller geometry designs can be achieved simultaneously (Ploeg & Foeth, 2013).

The above mentioned techniques have been proven in practice to improve the powering performance of a single screw ship significantly.

When a ship with single screw and symmetric hull form is already optimized, the remaining energy losses behind the ship is then the asymmetric slip-stream of the propeller which rotates only in one direction. The energy losses and the principle of the ship propulsion has been fully established by Wald (1965) and further elaborated by Dyne (1995) for practical considerations already. Recent studies (Dang et al., 2011 & 2012) have shown that both the transverse kinetic energy loss due to the swirl of the flow and also the axial kinetic energy loss due to the non-uniform axial velocity in the far field are the two major energy losses, that can be recovered by using ESDs.

However, ESDs often surfer from scale effects and fouling in full scale. Losing the stator blades in some cases and damaging the hull structure with cracks by ESDs have made the ship owners worried about applying ESDs to their ships.

The merit of applying an asymmetric aftbody lies in the fact that the swirl and the non-uniform flow of the ship's wake can be regulated in the same way as by applying ESDs in order to improve the interaction with a propeller, but without adding on additional 'appendages' to the hull. This idea is hence reviving recently.

Despite of the maneuvering problem of 'Carlotti', studied and tested at MARIN in the early 1950's that confirmed 15% shaft powering savings by applying an asymmetric aftbody (Collatz, 1985), many container ships with asymmetric aftbodies have been built in the 1980's (Stierman & Osborne, 1986). Some of the ideas of the asymmetric lines have been patented (Collatz, 1983, Piskorz-Nalecki, 1985, Nönnecke 1987 and Abramowski et al., 2010). Further studies went on into late 1980's and early 1990's (Stierman 1987, 1989, and Blaurock 1990).

It could be due to the difficulties in designing an asymmetric aftbody by using only model tests in the 1980's, and it could be also due to the difficulties in the ship's arrangement and construction, asymmetric aftbodies were not prevailing. However, the rapid growth of practical applications of CFD in hull form and propeller blade designs in the last decades opened a new era for applying asymmetric aftbodies where a fully-integrated hull-propeller design could be achieved to minimize the energy losses.

In this paper, the optimization procedure and its application to an Aframax tanker with asymmetric aftbodies are discussed in details. The resistance and self-propulsion tests have been carried out for the final optimized symmetric and asymmetric hull forms and more than 6% extra shaft power reduction has been obtained with an asymmetric aftbody. Cavitation observations and hull pressure fluctuation measurements have been conducted at MARIN's Depressurized Wave Basin (DWB) with the final designed propeller. Good cavitation performance and low pressure fluctuations on the hull have been measured. Maneuvering tests of the asymmetric hull has confirmed the normal maneuvering performance of the tanker, especially its course stability.

2 INTEGRATED HULL FORM AND PROPELLER DESIGN

2.1 Optimization by Massive CFD Calculations

The RANS code PARNASSOS, a code developed and frequently applied by MARIN, was used in the present study. It is dedicated to the prediction of the steady turbulent flow around ship hulls and solves the discretised Reynolds-Averaged Navier-Stokes equations (RANS) for steady incompressible flow. Various turbulence models are implemented in the code. For the present hull optimizations we used the Menter turbulence model. Structured multi-block grids are used with a finite-difference discretization of second and third-order schemes for the various terms.

This RANS code is coupled with a code based on Boundary Element Method (BEM) with potential flow simulation of propellers with blade sheet cavitation – called PROCAL. The coupling is done iteratively between the propeller loads and the volume forces for the RANS, until a self-propulsion has been found at given shaft power or speed. This technique is called RANS-BEM coupling.

The merit of this technique is that the induced velocity of the propeller can be calculated from the BEM code and subtracted from the total velocity field of the RANS calculations so that the effective wake field can be obtained. An effective wake field is essentially important for a good propeller design.

In order to optimize the hull form, parametric deformation of the hull form between some parent forms have been developed at MARIN by a computer code GMS-Merge where thousands of systematic hull forms can be easily interpolated between those parent forms. A similar deformation code has also been developed for the propeller geometry, which is fully parameterized in its main parameters and its radial distribution functions for the pitch, the chord, the camber, the thickness, the skew and the rake (Ploeg & Foeth, 2013). Thousands of propellers can be generated around a parent propeller or between parent propellers.

With thousands of hull forms combined with thousands of propeller geometry, a huge matrix of variations can be prepared for the CFD analysis. CPU and memory requirements of the PARNASSOS are quite modest compared to most other methods. A double-body computation for a single-screw ship on a mesh of about 2M cells takes only 2 hours on a single-processor PC. The BEM calculations consumes negligible amount of CPU time, even if with cavitation simulations. However for the hundreds of thousands of variations of hull forms and propellers, parallel computations are needed. At MARIN, the massive computations for all variants are distributed over a large number of idle desktop PCs at night, using the Condor tools. Typically, more than thousands of variants can be calculated over one night.

To judge the performance of the variants, various objective functions can be defined. For the power, either the resistance (the effective power) of the ship or the propeller shaft power can be used. For the wake field and comfort, either the uniformity of the wake (change of angle of attacks to the section profile of the propeller blades) or the pressure pulse levels can be used. For the present project, the shaft power at self-propulsion point in full scale and the variation of the angle of attacks of the section profiles of the propeller blades were used.

2.2 A case of symmetric form optimization

To illustrate how the integrated design of hull and propeller can improve the power performance of a ship in the design stage, a symmetric stern form has been discussed first for a single screw 78,000DWT bulk carrier.

This ship went first through a full optimization for the forebody with respect to both bow waves and also the viscous flow along the hull. With the same optimized forebody, three variants of aftbody have been proposed, being an extreme pram form, a moderate U-form and a classic V-form as the parent forms, see Figure 1.

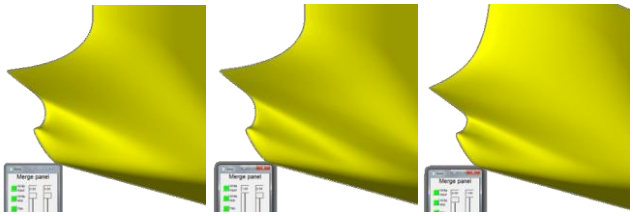

Figure 1: Three variants of the hull forms (from left to right: No. 1: an extreme pram form; No. 2: a moderate U-form and No. 3: a classic V-form).

By interpolation of the 3 parent hull forms with 10 steps between each two parents, $11 \times 11 = 121$ hull forms in total have been generated. With a selected stock propeller for this case, RANS-BEM coupling calculations have been carried out by distributing the calculations to all idle PCs at MARIN over night. 3.75 million cells have been used for each of the calculations.

When each of the calculation was converged, the self-propulsion at a given ship speed of 13.5 knots was achieved and the shaft power was obtained and used for the further comparison. To judge the quality of the wake field, a wake objective function (*WOF*) has been used, defined as,

$$WOF = \frac{2\int_{R_{hub}}^{R}\sqrt{\int_{\theta}(\partial V_A/\partial\theta)^2 d\theta}\,dr}{\pi(R^2 - {R_{hub}}^2)V_S} \qquad (1)$$

If we use the variant No. 1 as the basis for the comparison, a Pareto front can be built on the relative changes on the shaft power and the quality of the effective wake, see Figure 2.

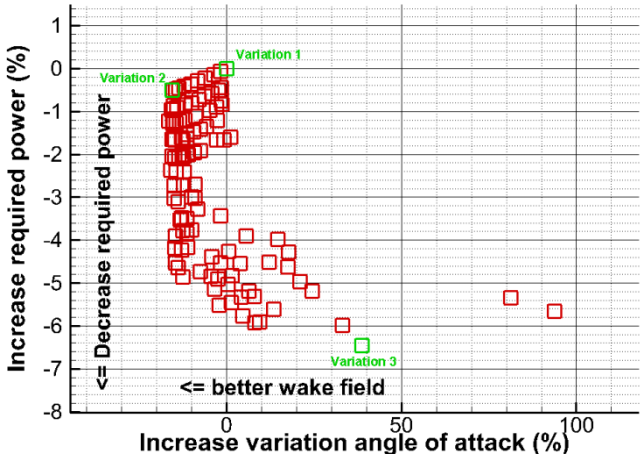

Figure 2: The Pareto front of a 78,000 DWT bulk carrier.

Not surprisingly, the classic V-form requires the lowest shaft power for the same ship speed, however with relatively worse wake quality for the propeller performance.

It can be seen however that a very good compromise can be easily found with the same wake quality as variant No.1 while with 5.5% lower shaft power. This hull form was finally chosen for a 78,000DWT bulk carrier.

As mentioned earlier, the merit of the RANS-BEM coupling for self-propulsion calculations is that the effective wake filed can be obtained by subtracting the induced velocity from the propeller. Figure 3 shows how the effective wake field looks like, which differs a lot from the nominal one that shows strong bilge vortices.

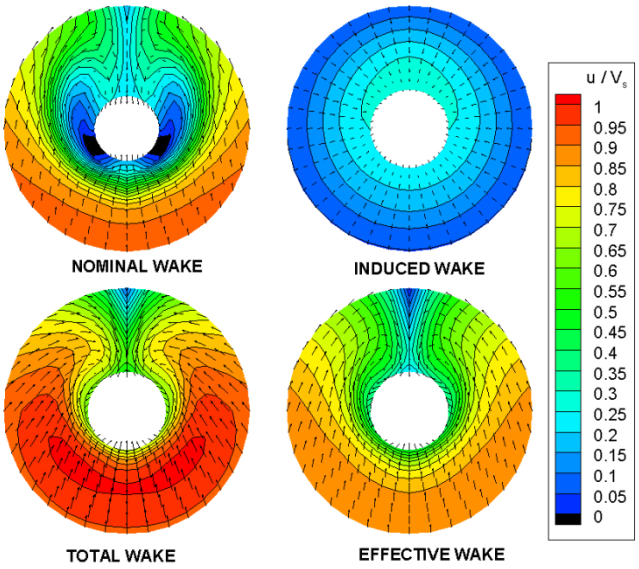

Figure 3: Calculation of the effective wake field.

3 ASYMMETRIC AFTBODY FOR AN AFRAMAX TANKER

The technique discussed in the previous section has been used for the development of the hull lines for an Aframax tanker for Guangzhou Shipyard International Company Ltd. (GSI), who are continuously searching for innovations for their ships. The idea for the present study was to make use of the technique to develop an optimal hull form with symmetric aftbody and used as the reference. In addition to the symmetric one, an asymmetric was optimized in the same way for full scale and would be verified by model tests, in order to investigate if further improvements on propulsive efficiency could be achieved.

3.1 Main Dimensions

The main dimensions of the ship is shown in Table 1.

Table 1: Main dimensions of the Aframax tanker.

	symmetric and asymmetric aftbodies		
	design draught	ballast draught	
L_{PP}	245.400	245.400	m
L_{WL}	250.000	237.570	m
L_{OS}	250.004	240.219	m
B	44.000	44.000	m
T_F	13.700	6.500	m
T_A	13.700	9.000	m

During the optimization, we kept the forebody identical to the optimized symmetric hull form and developed a few asymmetric aftbodies for this ship and used as the initial hull forms. Due to the difficulties to generate automatically hull forms at this moment by interpolations for asymmetric aftbodies, the interpolation between the initial hull forms was not carried out. The calculations with RANS-BEM coupling technique were only carried out for the initial hull forms. A simple comparison was made thereafter.

The best asymmetric initial hull form was selected after the RANS-BEM calculations which is compared to the symmetric one in Figure 4, where the asymmetric aftbody is designed for a right-handed propeller. In order to prevent possible maneuvering problem and also in believe that the hull form far upstream does not contribute too much to the flow at the stern, the asymmetric form has only be applied to the gondola of the ship. The main hull remained the same for both symmetric and asymmetric ships.

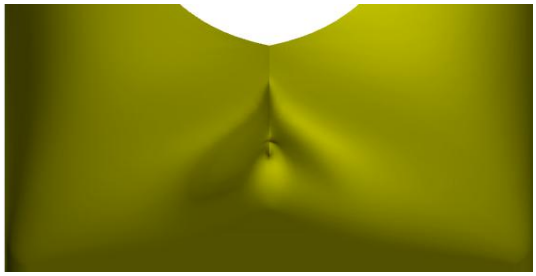

symmetric aftbody

asymmetric aftbody

Figure 4: Symmetric and asymmetric aftbodies.

3.2 CFD Analyses with RANS-BEM Coupling

The computational domain is shown in Figure 5 and the main dimensions of the domain size are given in Table 2. In total, 7.7 and 5.7 million cells have been used for full-scale and model-scale calculations, respectively.

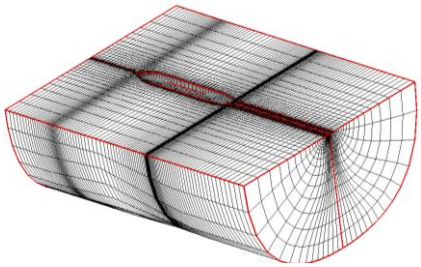

Figure 5: The computational domain (number of visualised grid cells is reduced by a factor of four in all directions).

Table 2: Main characteristics of the domain for full / model scale calculations.

Inflow (distance in front of bow)	0.5 L_{PP}
Left exterior	1.0 L_{PP}
Bottom	deep (1.5 L_{PP})
Outflow (distance behind transom)	1.0 L_{PP}
Type of grid	Structured multi block
Number of blocks	2
Number of hull surface elements	about 22400
Number of Grid Cells	about 7.7 / 5.7 million

Multi-block structured grids for the RANS calculation around the hull were used. Figure 6 shows the grids on a sections along the aftbody. In order to avoid grid dependency of the calculation results, the grids for all variants studies were created by using the same parameters. The potential based panel method was used for the simulation of the propeller flow where 60 (chord wise) × 30 (radial direction) panels were used, see Figure 7.

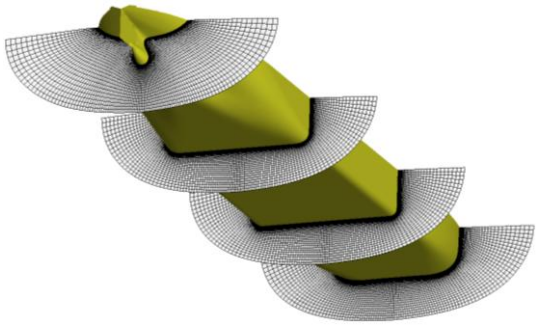

Figure 6: Stern view of various slices of the structural grid along the hull.

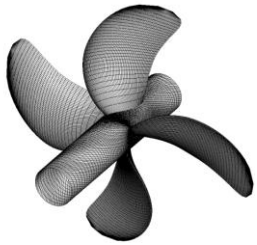

Figure 7: Panel distribution on the propeller.

The level of convergence and y+ values that were obtained both for the nominal (without an operating propeller) and the total (with a propeller in operation) computations, respectively, and listed in Table 3 and Table 4.

Table 3: Convergence level of solution – without propeller.

	model scale		full scale	
	symmetric	asymmetric	symmetric	asymmetric
Convergence	1×10^{-5}	1×10^{-5}	1×10^{-5}	1×10^{-4}
Y+ max	0.23	0.37	0.50	0.30

Only local points at the symmetric plane have slightly higher values.

Table 4: Convergence level of solution – with propeller.

	model scale		full scale	
	symmetric	asymmetric	symmetric	asymmetric
Convergence	1×10^{-4}	1×10^{-4}	1×10^{-4}	1×10^{-4}
Y+ max	0.24	0.90	0.25	0.25

Only local points at the symmetric plane have slightly higher values.

As the first assessment on the effectiveness of the asymmetric aftbody on improving the propulsive efficiency, the nominal wake fields have been studied in model scale. The measured and calculated wake fields are shown in Figure 8. Both results show that a very strong pre-swirl, against the rotational direction of a right-handed propeller, has been successfully generated by the selected asymmetric aftbody. The CFD calculation results agree very well with the experimental data, measured with 5-hole Pitot tubes.

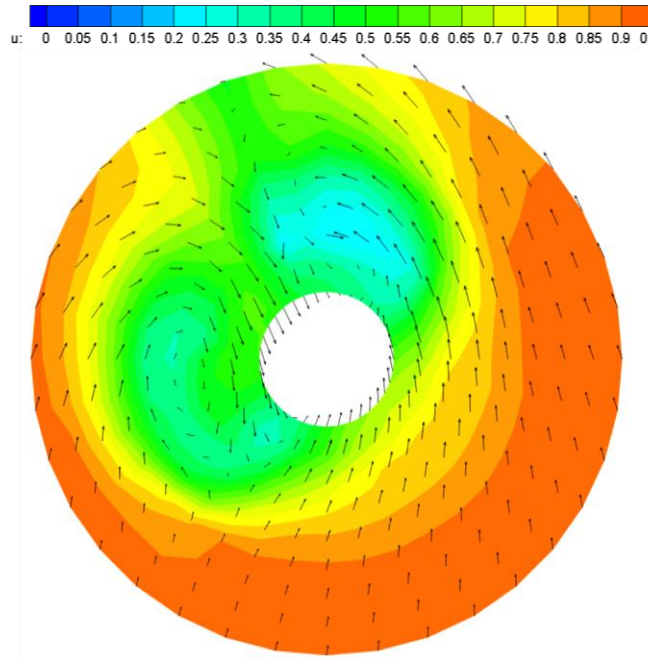

measured wake

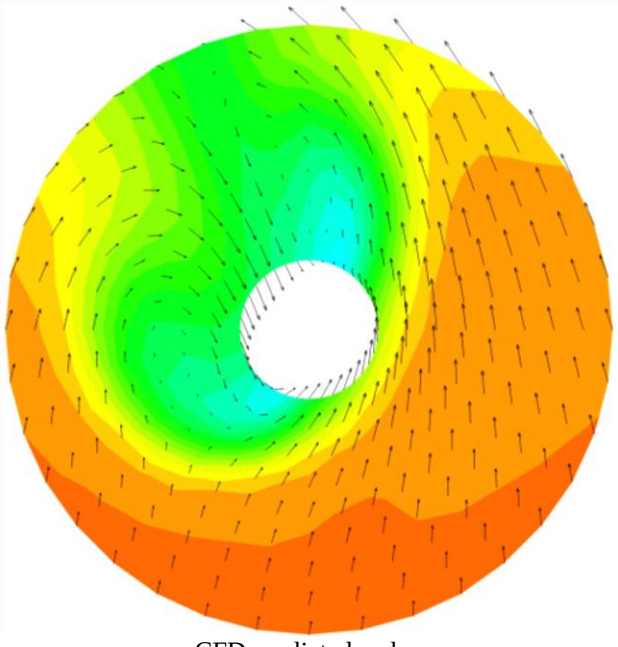

CFD predicted wake

Figure 8: Comparison of the measured nominal wake and the calculated nominal wake in model scale (at design draught and speed).

Two strong bilge vortices are clearly seen in the nominal wake field, however weakened significantly when a propeller is in operation. These can be seen by the plots in Figure 9 where both the effective wake fields of the symmetric aftbody and the effective wake fields of the asymmetric aftbody are shown for both model-scale and full-scale Reynolds numbers.

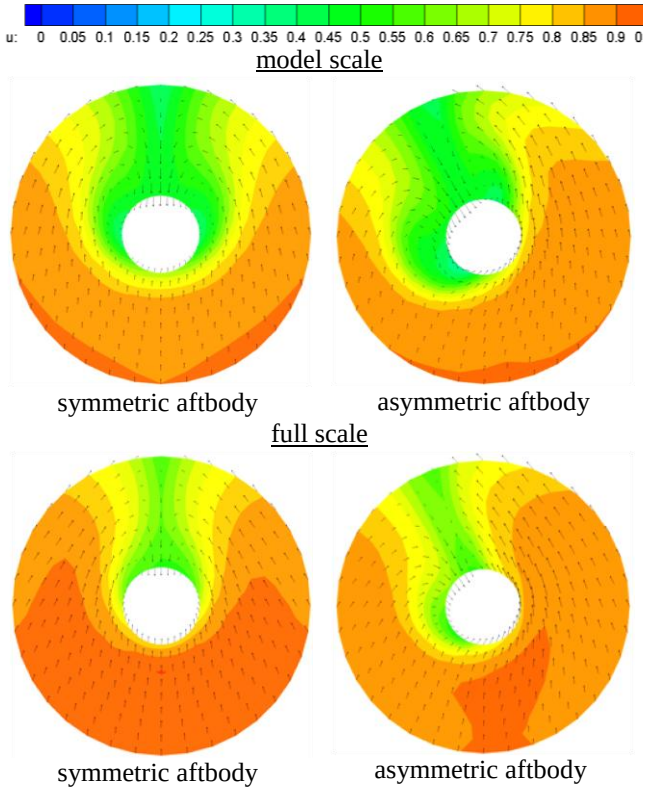

Figure 9: Comparison of the effective wake fields in model and full scales; and the symmetric and asymmetric aftbodies (at design draught and design speed).

Scale effects are clearly seen between the model-scale and full-scale wake fields, especially the axial components. The pre-swirl generated by the asymmetric aftbody remains more or less the same for both scales.

3.3 Wake Fields and Kinetic Energy

Although the shaft power can be calculated directly by the RANS-BEM coupling technique and assessed for the ship's powering performance, as shown in Figure 2, the kinetic energy losses in the ship's far wake field, where the static pressure is completely recovered, provide indirect but easy assessment on the propulsive efficiency and a better illustration of the velocity field. The complete theory can be found in Wald (1965), however the kinetic energy losses the wake can be simplified into Equation (2) to (4),

$$K_{ax} = \int_{S_w} \frac{V_a}{V_s}\left[\left(1-\frac{V_a}{V_s}\right)^2\right] ds/S_w \quad (2)$$

$$K_{tr} = \int_{S_w} \frac{V_a}{V_s}\left[\left(\frac{V_t}{V_s}\right)^2 + \left(\frac{V_r}{V_s}\right)^2\right] ds/S_w \quad (3)$$

$$K_{total} = K_{ax} + K_{tr} \quad (4)$$

where the total kinetic energy losses are split into the axial part K_{ax} and the transverse part K_{tr}.

It might be not a bad idea to make the assessment of the kinetic energy losses just behind the propeller, as shown by the 'behind wake disc' in Figure 10, instead of the real far field where numerical dissipation may become too strong. Although the static pressure just behind the propeller is not completely recovered, it is assumed that the difference between the symmetric hull and the asymmetric hull may not differ too large. The kinetic energy difference at that location may provide important information on the energy saving by applying an asymmetric aftbody in a relative sense.

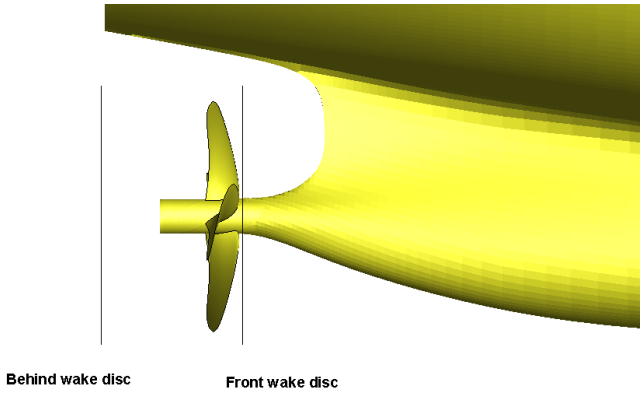

Figure 10: Locations of the wake fields studied.

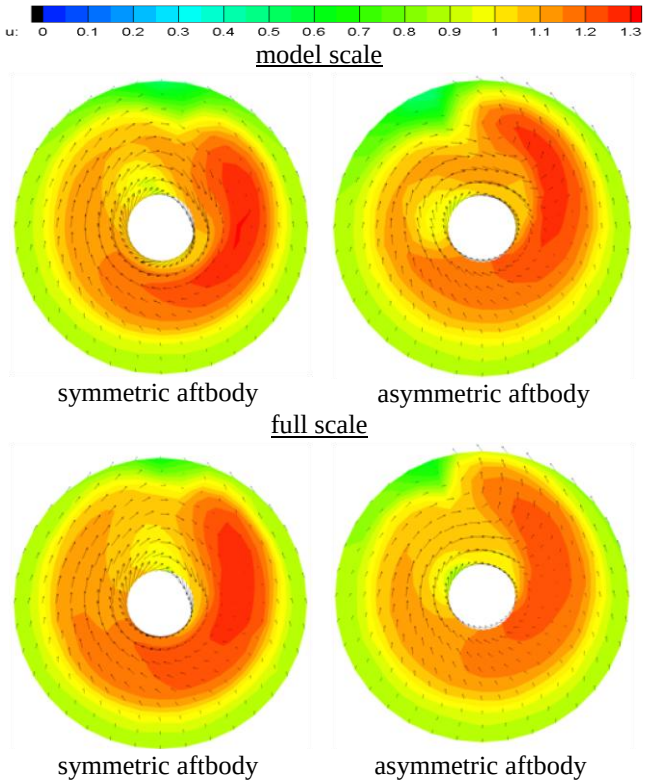

Figure 11: Comparison of the total velocity fields in model and full scales, symmetric and asymmetric aftbodies (at design draught and design speed).

On the 'behind wake disc' with an operating propeller at self-propulsion condition, the velocity wake fields are compared to each other between the symmetric and the asymmetric aftbodies for both the model-scale and the full-scale in Figure 11.

Two major phenomena are shown in those plots: compared to the symmetric aftbody, the axial velocity field becomes more uniform for the asymmetric aftbody, especially the reduction of the peak on the starboard side where the propeller blades rotate downwards; on the portside, the tangential velocity is reduced significantly by the asymmetric aftbody.

The axial and transverse kinetic energies on the 'far field domain' as defined in Figure 12 at the 'behind wake disc' location shown in Figure 10, can be integrated by using Equation (2) to (4) to make quantitative assessments on the kinetic energy losses. This can be done both for a ship without a propeller (resistance test situation) and for a ship with an operating propeller (self-propulsion situation).

In order to prevent truncation errors during numerical integration, instead of using the large domain *B* in Figure 12, a small domain *A* in the same figure was used in order to focus on the flow around the propeller disc. The results are compared between the symmetric and asymmetric aftbodies in Table 5 and Table 6 for the ship in resistance and in self-propulsion conditions, respectively.

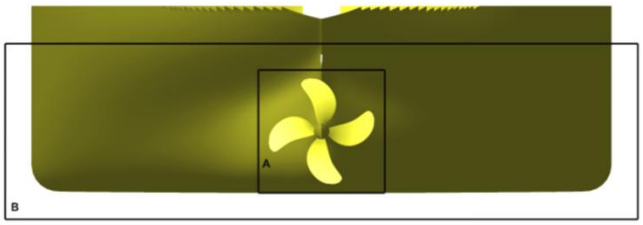

Figure 12: definition of the 'far field' domain *A* for kinetic energy integration, looking from the stern to the bow.

Table 5: Comparison of kinetic energy, resistance.

	model scale			full scale		
	sym.	asym.	%	sym.	asym.	%
K_{ax}	0.0343	0.0337	-1.75	0.0167	0.0166	-0.60
K_{tr}	0.0054	0.0074	+37.04	0.0049	0.0071	+44.90
K_{total}	0.0397	0.0411	+3.53	0.0216	0.0237	+9.72

It can be seen from Table 5 that the transverse kinetic energy losses behind the ship without a propeller are much smaller than that of the axial kinetic energy losses, both in model and full scales. This indicates that the major energy loss in the nominal wake of a ship is the axial kinetic energy loss. In addition, the axial kinetic energy loss in full scale is lower than that in model scale, as is expected, and is about only half of that in the model scale for the present ship.

The transverse kinetic energy losses are increased when the asymmetric aftbody is applied, indicating that pre-swirl does cost extra energy. This increase has been found both for model and full scales, and with almost the same amount.

This could mean that the pre-swirl generated by an asymmetric aftbody is less Reynolds dependant.

The total kinetic energy losses in the small domain A in model scale is only 3.53%, indicating that the asymmetric aftbody may not generate noticeable resistance increase in model scale during a resistance test.

Table 6: Comparison of kinetic energy, self-propulsion.

	model scale			full scale		
	sym.	asym.	%	sym.	asym.	%
K_{ax}	0.0211	0.0220	+4.27	0.0220	0.0182	-17.27
K_{tr}	0.0331	0.0238	-28.10	0.0245	0.0148	-39.59
K_{total}	0.0542	0.0458	-15.50	0.0465	0.0330	-29.03

When studying the kinetic energy losses behind an operating propeller during a self-propulsion condition, it is clearly seen that the transverse kinetic energy losses are increased due to the rotational flow in the slip stream of the propeller, to a level more or less the same as or even higher than the axial kinetic energy losses in the wake, see Table 6. Significant reduction of the transverse kinetic energy losses by applying the asymmetric aftbody has been calculated both in model scale and in full scale in Table 6.

Finally, total reductions of the kinetic energy losses of about 15.5% in model scale and about 29.0% in full scale have been found by the asymmetric aftbody. The reduction of the kinetic energy in full scale doubles almost that in model scale. This may indicate more energy saving in full scale than in model tests, as already experienced in full scale trials by Collatz (1985).

Further illustration of the reduction of the kinetic energy losses in the wake by applying an asymmetric aftbody can be done by comparing the total viscous velocity field to that of the potential field where energy along each streamline is conserved. Such a comparison is plotted in Figure 13. The figure shows that the axial velocity deficit (due to viscous effects) or increase (due to propeller actuation) behind the asymmetric aftbody is less than that of the symmetric one.

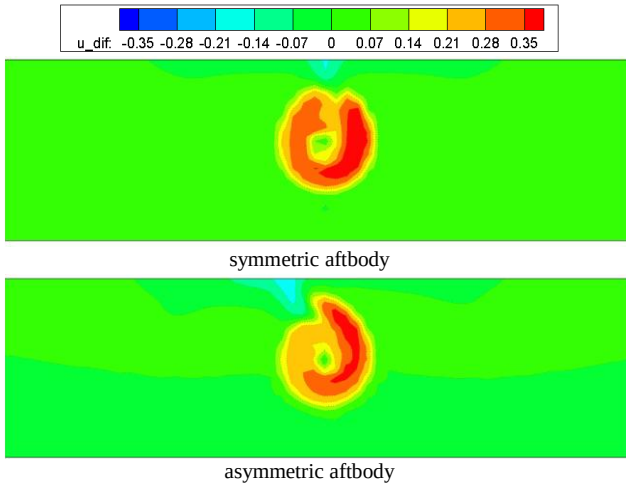

Figure 13: Total velocity differences from the potential flow in the 'far field' – full scale .

3.4 Resistance and Propulsion tests

To verify the CFD calculations for energy saving by applying an asymmetric aftbody, large ship models to a scale of 1:25.717 have been built for the tanker, which consists of one forebody and two aftbodies – symmetric and asymmetric, connected at station 10.

Two resistance tests have been carried out at design and ballast draughts for both the symmetric and asymmetric aftbodies. The results are extrapolated to full scale with the same correlation factors and compared in Figure 14.

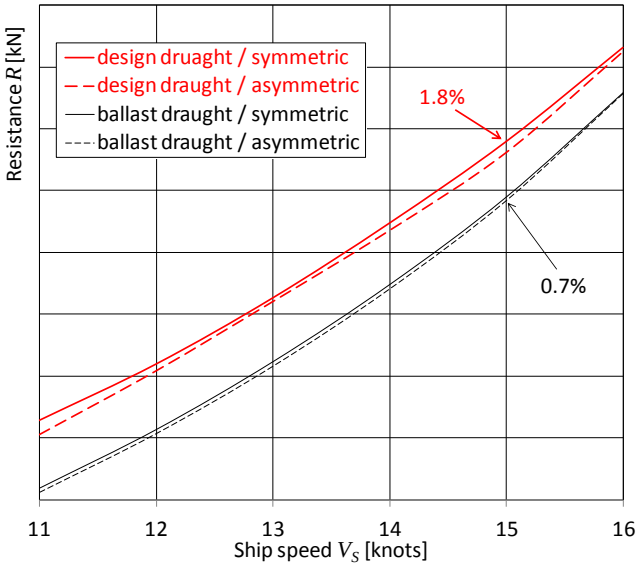

Figure 14: Comparison of the total resistance of the ship at design and ballast draughts, extrapolated to the full scale with the same form factor and correlation factors for each draught.

It is very similar to the test results of other asymmetric ships developed in the 1980's (Collatz, 1983 and 1985) that slightly lower resistance has been measured in both draughts for the present ship with an asymmetric aftbody. Although it cannot be generalized that an asymmetric aftbody can always reduce the ships resistance, both the kinetic energy analyses (Table 5) and the resistance tests (Figure 14) show that an asymmetric aftbody has limit effect on the ship's resistance in model scale.

By assuming that the amount of viscous wake, which goes through the propeller disc, is the same for the symmetric and asymmetric aftbodies, the same wake scaling can be used in the extrapolation of the self-propulsion test results. The speed-power-RPM relations are obtained and plotted in Figure 15 for the design draught to compare the performance of the symmetric and asymmetric aftbodies. About 6.6% shaft power savings have been found by the asymmetric aftbody.

It should be pointed out that the findings in Table 5 that an asymmetric aftbody may result in even less kinetic energy losses and more savings in full scale than in model scale is

not taken into account in the present extrapolation. In order to take this effect into consideration, correlations to full scale trial data are needed. At this moment, information on full scale trials of asymmetric ships is very scarce.

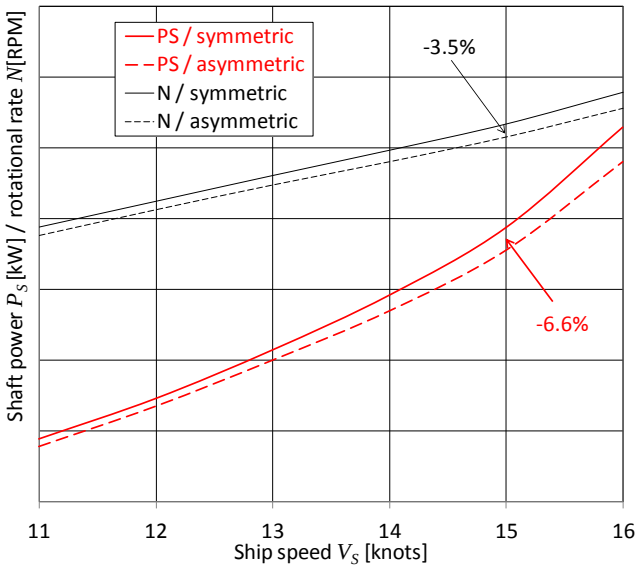

Figure 15: Shaft power savings and shaft rotational rate changes due to asymmetric aftbody (at design draught).

3.5 Cavitation and Pressure Fluctuation

To judge the cavitation performance of the propeller operating behind the present Aframax tanker with an asymmetric aftbody, cavitation observations and hull pressure fluctuation measurements were carried out with the final design propeller at MARIN's Depressurized Wave Basin (DWB), which measures 250m long, 18m side and 8m deep. Two high speed video cameras, looking through windows from the hull model on both starboard and port side were used to record the cavity pattern and their dynamics during growth and collapse. Strong illumination through a Perspex block above the model propeller was necessary in order to obtain high frame rates with good quality of the video recordings, see the photo in Figure 16.

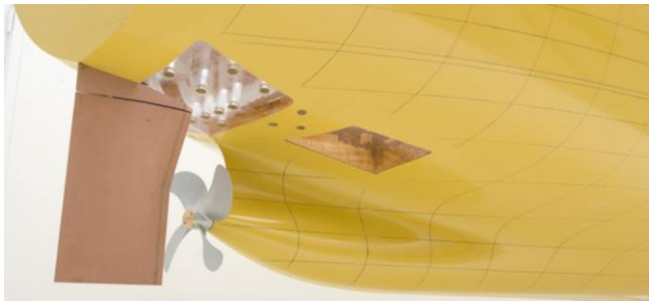

Figure 16: The Perspex block for illumination and the observation window for the high speed video cameras.

Cavitation observations have been carried out both in design draught and ballast draught conditions. The most developed cavitation on the propeller blades was observed at ballast trial condition with 85% MCR power. The selected screenshots of the high-speed video recordings at this condition are shown in Figure 17, looking from both starboard and portside simultaneously.

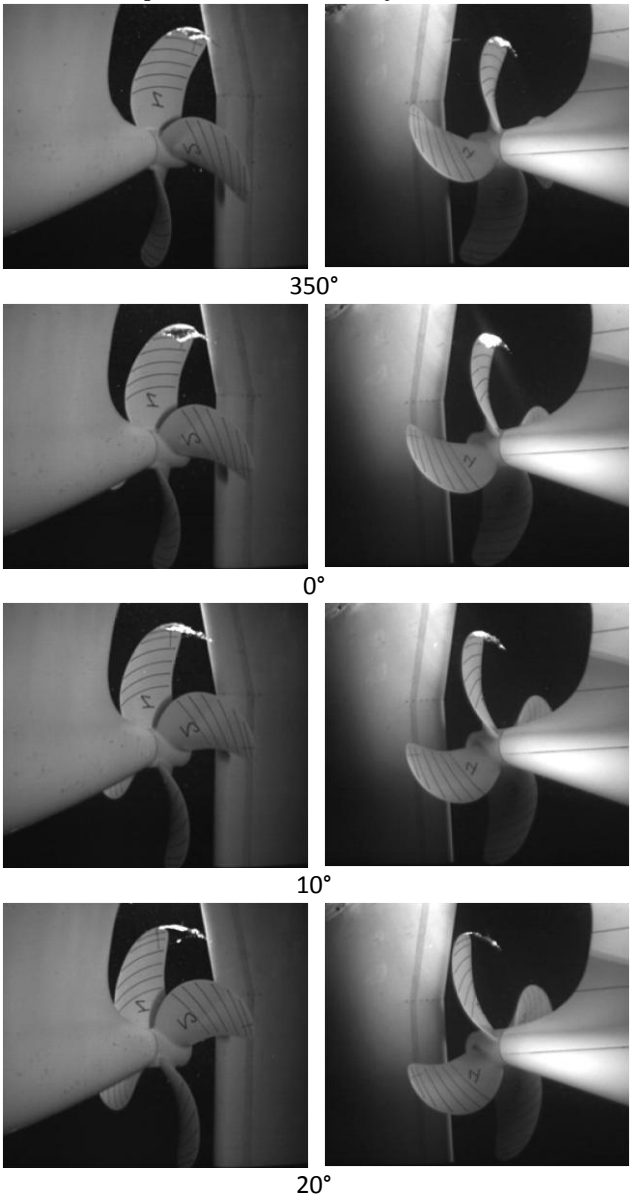

Figure 17: Screenshots of the high speed video recordings (3000fps) of the cavity patterns on the propeller blades at various angular positions when blade No. 1 passing through the 12 o'clock position of the wake (ballast draught, 85% MCR power and ideal trial condition).

It can be seen from the video recordings that the sheet cavity develops and collapse smoothly toward the tip to connect with and develop into the tip vortex cavitation. The largest extend of the cavity in the ballast condition occurred around 12 o'clock position and covered only the area from 0.9R to the tip. Compared to similar ships with symmetric aftbodies, this amount of cavitation at ballast condition is judged to be small. No cavitation erosion on the design propeller blade will be expected.

The cavity on the propeller blade at design draught is smaller and very limited, and will not be discussed here.

To measure the pressure fluctuation on the hull surface in order to judge the excitation forces on the hull surface by cavitation, a matrix of 20 pressure pick-ups have been used during the model tests. Figure 18 shows the pressure pick-up arrangement.

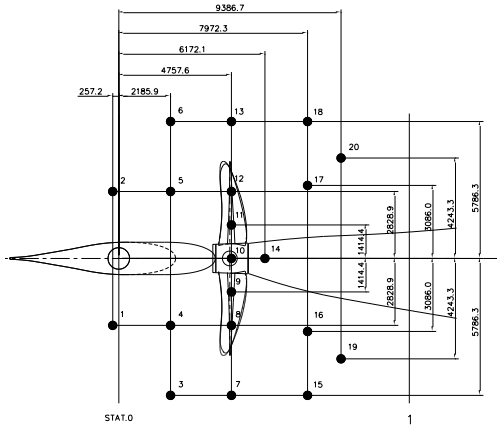

Figure 18: Arrangement of the pressure pick-ups.

Since the stern hull plate is completely out of the water at ballast condition, it is only meaningful to measure the excitation force when the stern is wet. The measured hull pressure fluctuations on the surface above the propeller are shown in Figure 19 at the design draught and the design speed with 85% MCR power in service condition with 15% SM for the first four blade harmonics. The highest pressure fluctuation has been recorded at pick-up No. 14 with an amplitude of only 1.18kPa for the blade frequency. The higher harmonics are virtually zero.

To make an assessment on the propeller excitation on the possible hull vibration, the pressure fluctuation on the hull surface on the stern is integrated into a vertical excitation force, taken into considerations of the phase difference at different pressure pick-ups.

The integrated equivalent vertical excitation force at this condition is less than 20 kN, as shown in Table 6, which is way below the criterion of van der Kooij that reads:

$$F_{Zeq} = \sqrt{\left(\sum iF_{Z-i}\right)} < c\nabla(0.75 + 75/L), i = 1\ to\ 4 \quad (5)$$

where c is an empirical constant depending on the type of ship, its aftbody construction and whether or not the accommodation is located above the propellers. For the present tanker a value of 5 was taken; ∇ is the displacement volume of the ship in m^3; L is the length between perpendiculars in m and $F_{Z\text{-}i}$ is the amplitude of the i-th harmonic component of the vertical excitation force.

Table 7 shows that the measured hull excitation remains far below the criterion and it is therefore concluded that the propeller-induced hull excitation is very low. Hence, no vibration problems are expected, provided that resonance of the ship's structure does not occur.

Table 7: Integrated vertical excitation force F_{Zeq}.

Condition	F_{Zeq} measured	F_{Zeq} allowed
Design draught, 85% MCR service condition, 15% SM	19.5 kN	619.8 kN

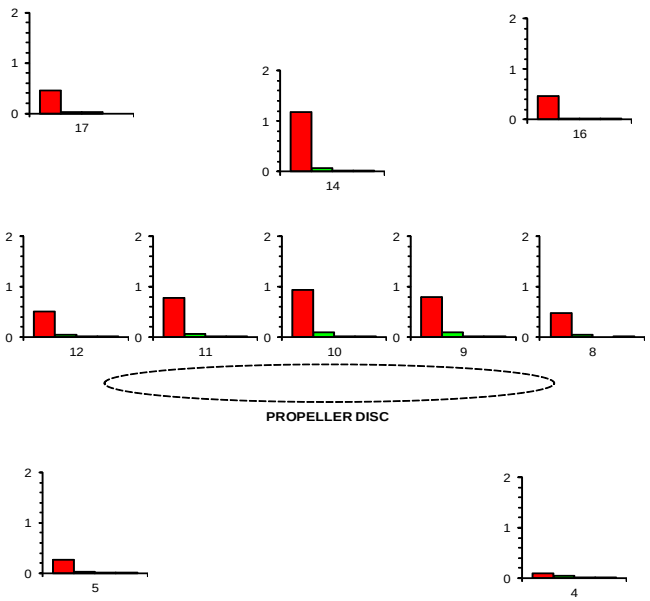

Figure 19: The hull pressure fluctuations above the propeller at design draught and service speed with 85%MCR power.

3.6 Course Stability

As known and mentioned earlier in this paper, the maneuverability of a ship with asymmetric aftbody was one of the worries for the shipyards and the owners, especially with regard to ship's course stability. The efficiency gained from asymmetric aftbody in ideal straight course can easily be diminished or completely cancelled if the ship needs continuously to steer in order to keep a straight course.

To determine the maneuvering characteristics, standard zig-zag and combined turning circle / pull-out experiments were conducted. Additional turning circles and very small zig-zag maneuvers were carried out to determine the stability curve.

The standardized maneuvering derivatives have been verified where relevant with the criteria as posed by the IMO in their resolution MSC. 137(76) have been compared to the values of similar ships in the MARIN maneuvering database (see Figure 20 and Figure 21). These similar vessels were selected looking at the type of vessel and steering/propulsion unit.

The approach speed during these tests was 13.5 knots.

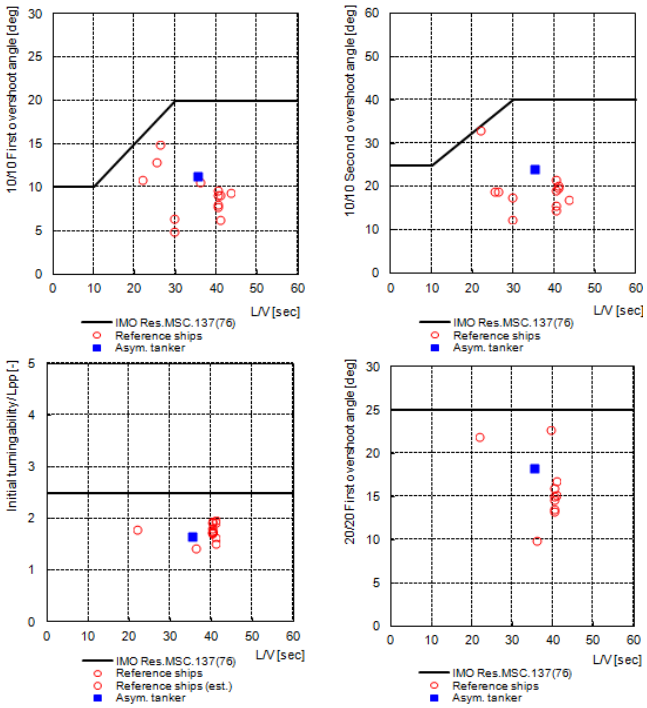

Figure 20: Zig-zag maneuver performance of the Aframax.

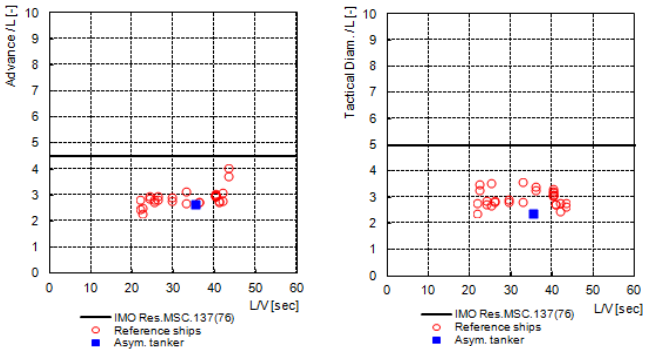

Figure 21: Turning circle performance of the Aframax.

The direct spiral test results, i.e. the plot of angular velocity versus steering angle, were determined by means of combined turning circle / pull-out tests at different steering angles, as shown in Figure 22.

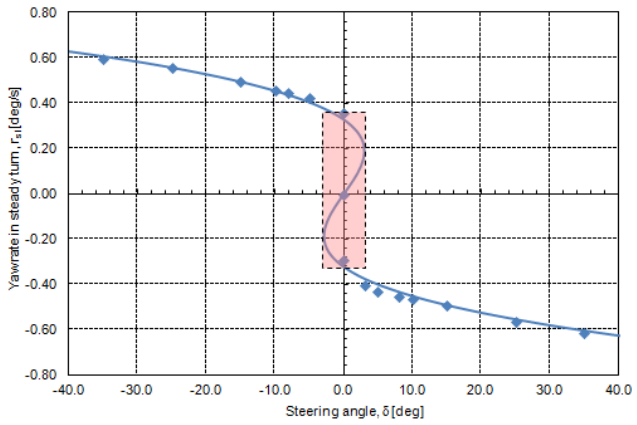

Figure 22: Rate of turn as function of steering angle.

The width on instability loop was verified by means of additional very small zig-zag maneuvers. The time histories of the very small zig-zag maneuvers show that the vessel reacts less and less to the provided steering angles from 6 to 2 degrees. Based on the spiral tests and very small zig-zag maneuvers, it can be concluded that the width of instability loop is about 5 degrees.

It has to be noted that a ship does not necessarily need to be directional stable in any situation to be operational safe and efficient, therefore some instability is fully acceptable.

Based on the comparison presented in the figures, it can be concluded that the ship complies easily with the IMO resolution MSC. 137(76) concerning the yaw checking and course keeping abilities, the initial turning ability and the turning ability.

4 CONCLUDING REMARKS

In the past decades, completely integrated hull lines and propeller design methodologies have been developed at MARIN to optimize the total propulsive efficiency and comfort of a ship hull-propulsor system. With the aid of the RANS-BEM coupling technique, massive calculations can be carried out over a single night for thousands of systematical variations of hull lines and propeller geometry which are interpolated between parent hull forms and propeller geometries.

By applying asymmetric aftbody to further reduce the kinetic energy losses in the ship far wake, a full integration of the hull form and the propulsor is realized.

The design exercise carried out for an Aframax tanker for GSI with a moderate asymmetric aftbody, where only the gondola is made asymmetric, shows that an extra propeller shaft power reduction of about 6.6% can be achieved with respect to an already-optimized symmetric hull form with identical forebody. Somewhat higher shaft power reduction can be expected in full scale trials based on the CFD calculation results and the wake kinetic energy analyses.

The cavitation observations with high speed video's show stable and healthy cavitation on the final propeller design with very limited amount cavitation on the blade. The pressure fluctuation on the hull surface is lower than the normal level for similar ships.

The extensive maneuvering tests of this Aframax tanker with asymmetric aftbody show normal or better maneuvering performance than similar ships, especially for the course stability. This removes that concern on the maneuvering performance of a ship with an asymmetric aftbody.

It is the authors wish in the future that systematic hull form variations, interpolated from parent asymmetric hull forms, can be automatically generated so that massive RANS-BEM self-propulsion calculations can be carried out to further optimize the design process in asymmetric aftbody designs.

ACKNOWLEDGMENTS

The authors are grateful for the valuable support from Guangzhou Shipbuilding International Company Ltd. (GSI) for the present study. Thanks are also extended to Roberto Tonelli of MARIN for carrying out the maneuvering tests and making the assessments on the maneuverability of this Aframax tanker, especially its course stability.

REFERENCES

Abramowski T., Żelazny K. and Szelangiewicz T., (2010). Numerical analysis of effect of asymmetric stern of ship on its screw propeller efficiency. Polish Marine Research, Vol. 17, pp. 13-16.

Blaurock J., (1990). An appraisal of unconventional aftbody configurations and propulsion devices. Marine Technology, Vol. 27, No. 6, Nov., pp. 325-336.

Collatz G., (1983). Fuel saving by asymmetric afterbodies for single screw vessels. Journal of Ocean Engineering - Vol. 10, No. 4, pp. 213-226.

Collatz G., (1985). Non-symmetrical aft-bodies. Proceedings of Workshop on Developments in Hull Form Design, 22-24 October, Wageningen, The Netherlands.

Dang J., Chen H., Dong G., van der Ploeg A., Hallmann R. and Mauro F., (2011). An exploratory study on the working principles of energy saving devices (ESDs), Greenship'2011, Wuxi, China.

Dang J., Dong G. and Chen H., (2012). An Exploratory Study on the Working Principles of Energy Saving Devices (ESDs) – PIV, CFD Investigations and ESD Design Guidelines, OMAE 2012, paper No. OMAE2012-83053.

Dyne G., (1995). The Principles of Propulsion Optimization, Transactions RINA, 137, pp. 189-208.

Nönnecke E.A., (1987). Schiffe mit treibstoffsparendem asymmetrischen Heck-Anwendungen und Erfahrungen. Schiff und Hafen/Kommandobrücke, No. 9.

Oosterveld M.W.C., (1970). Wake Adapted Ducted Propellers. PhD Dissertation of Delft University of Technology.

Piskorz-Nalecki J. W., (1985). The influence of the asymmetric afterbody and the horizontal fins on the rudder blade on the propulsive efficiency. Proceedings of Workshop on Developments in Hull Form Design, 22-24 October, Wageningen, The Netherlands.

van der Ploeg A. and Raven H.C., (2010). CFD-based optimization for minimal power and wake field quality. Proceedings of 11th International Symposium on Practical Design of Ships and Other Floating Structures (PRADS), Rio de Janeiro, Brazil.

van der Ploeg A. and Foeth E-J., (2013). Optimization of a chemical tanker and propeller with CFD. Proceedings of ECCOMAS International Conference on Computational Methods in Marine Engineering V, Hamburg.

Stierman E.J., (1987). The design of an energy saving, wake adapted duct. Proceedings of Int. Symposium on Practical Design of Ship and Other Floating Structures (PRADS'87), Trondheim, Norway.

Stierman E.J., (1989). Energy saving with an asymmetric stern and wake adapted ducts. Proceedings of Int. Symposium on Ship Resistance and Powering Performance, Shanghai, China April 11-14, p.124-132.

Stierman E.J. and Osborne M.G., (1986). A review of the performance and application of the asymmetric stern. Shell International Marine, SIM Report No. MR 13/86.

Wald, Q., (1965). Performance of a propeller in a wake and the interaction of propeller and hull, Journal of Ship Research, Vol. 9, June, p 1-8 & 36.